

# Flow phenomena and stability of microfluidic networks

**Problem presented by**

John Melrose and Guoping Lian

*Unilever Research*

**Problem statement**

Steady two-phase flow in a microfluidic device is examined using a network model. The generalisation of Kirchhoff's laws from electric-circuit theory to two-phase flow is demonstrated assuming no-slip between the phases. Missing equations at nodes can be replaced by realistic physical assumptions based on how the phases divide at these junctions. The stability of large parallel microfluidic devices to manufacturing tolerances is also examined and extensions to the model for future work are suggested.

**KEYWORDS:** network, multiphase, nodal laws, droplets, meniscus, Kirchhoff laws.

**Study Group contributors**

John Billingham (University of Nottingham)  
Andrew Grief (University of Oxford)  
John Hinch (University of Cambridge)  
David Leppinen (University of Cambridge)  
Shailesh Naire (Heriot-Watt University)  
John Ockendon (University of Oxford)  
Nick Ovenden (University College London)<sup>1</sup>  
Howell Peregrine (University of Bristol)  
Colin Please (University of Southampton)  
Jean-Marc Vanden-Broeck (University of East Anglia)  
Gorden White (University of Oxford)  
Eddie Wilson (University of Bristol)

---

<sup>1</sup>Corresponding author, email [nicko@math.ucl.ac.uk](mailto:nicko@math.ucl.ac.uk)

## Report prepared by

John Billingham (University of Nottingham)  
Andrew Grief (University of Oxford)  
David Leppinen (University of Cambridge)  
Nick Ovenden (University College London)

# 1 Introduction

Microfluidics is a relatively new and fast growing research area in fluid mechanics. The devices in question are thin wafers containing etched or printed interconnecting channels through which fluids are pumped, which can mix and/or react at various nodes to produce an output *product*. Microfluidic devices have applications in many manufacturing and chemical detection processes. For example, they can be used to manufacture monodisperse droplets with very well defined properties for pharmaceutical applications; or form the basis for miniaturised ‘*lab-on-a-chip*’ sensor arrays for detecting biological substances or toxins. The potential applications include pharmaceuticals, biotechnology, the life sciences, defence, public health and agriculture (Ouellette, 2004). An excellent review of the current state knowledge is given by Stone et al. (2004).

The particular problem posed by Unilever to the 49th European Study Group with Industry concerns the formation and transport of droplets in an interconnected network of microchannels. Two streams, one of oil and one of water, feed into the device network and interact, producing oil droplets of a controlled size as the output. This problem in microfluidics is closely related to multiphase transport in porous media (see the reviews by Olbricht, 1995; Payatakes, 1982).

For manufacturing processes, Unilever wishes to parallelize massively a process such as droplet formation with a large number of output channels producing droplets of equal size. However, their experiments reveal that instabilities in the flow pattern lead to some output channels containing single-phase flow or at least inconsistent droplet formation. Unilever would like to understand what network design features lead to such behaviour. A further related question is how to make such a network robust, in order that fouling and blocking of one part of the system will not have catastrophic consequences on the entire manufacturing process.

From our discussions with Unilever, we have attempted to address the following issues in this report:

- The generalisation of Kirchhoff’s laws of mass conservation and momentum (electric-circuit theory) to multiphase (immiscible) steady flows in complex networks of channels and nodes.
- The sensitivity of instabilities to the tolerances of chip manufacture (principally channel width). What tolerances are required to suppress these instabilities?
- Advice on design principles to give robustness to the network.

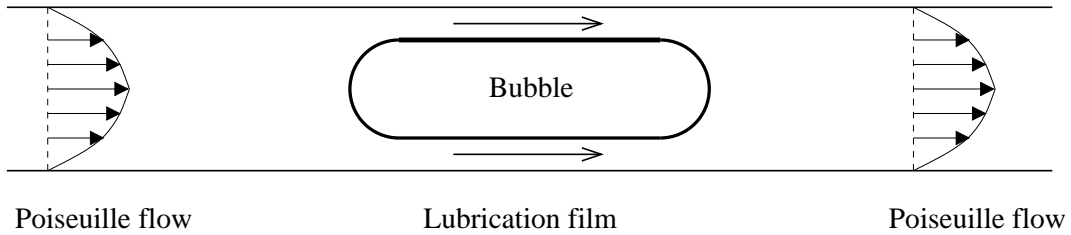


Figure 1: A bubble flowing through a capillary tube highlighting the Poiseuille flow upstream and downstream of the bubble and the lubrication film between the bubble and the tube wall.

## 2 Droplet dynamics

A paper of fundamental importance to modelling the transport of droplets in microchannels is by Bretherton (1961) who studied the motion of bubbles in capillary tubes (figure 1). It is assumed that a bubble with mean diameter much greater than that of the capillary tube is immersed in a liquid and that there is an imposed pressure gradient. Far upstream and downstream of the bubble the flow in the liquid can be modelled as Poiseuille flow. In between the bubble and the capillary tube walls there will be a thin layer of liquid. There are large forces associated with this thin lubrication layer and there is a net pressure drop across the bubble which is proportional to  $Ca^{2/3}$ , where  $Ca$  is the Capillary number. Thus, Bretherton (1961) was able to show that the total pressure drop within the capillary is the sum of a pressure drop associated with the Poiseuille flow away from the bubble and a pressure drop due to lubrication forces near to the bubble. Subsequently Hodges et al. (2004) has extended Bretherton's work by examining the flow around a viscous drop in a capillary. Hazel and Heil (2002), Wong et al. (1995a) and Wong et al. (1995b) further extended the work of Bretherton by examining flow within non-circular tubes, while Borhan and Mao (1992) considered the influence of surfactants.

Manga (1996) examined the dynamics of drops in branched tubes using a boundary integral technique. He examined the case of a single tube branching into two tubes and he showed that the likelihood of drops entering the high-flow-rate branch increases as (i) the viscosity ratio between the drops and suspending fluid decreases, (ii) the capillary number  $Ca$  increases, and (iii) the drop size increases. Stark and Manga (2000) developed a model to track the motion of bubbles within a network of tubes of varying radius. Their model included the effect of pressure drop within capillary tubes due to both Poiseuille flow in the suspending fluid and due to the so-called Bretherton effect. They also examined the effect of different nodal laws to specify the path taken by a bubble at the junction between branching tubes. Manga (1996) developed a network model to examine how the hydraulic conductivity of an interconnected network of tubes is influenced by the presence of bubbles. Their model identified critical flow paths which amplify fluctuations in the hydraulic conductivity and hence fluid flow.

The breakup of a droplet at a constriction in a capillary tube is of considerable relevance to oil recovery and has been extensively studied by Payatakes (1982); Olbricht and Kung (1992); Borhan and Pallinti (1999); Tsai and Miksis (1994, 1997) for example.

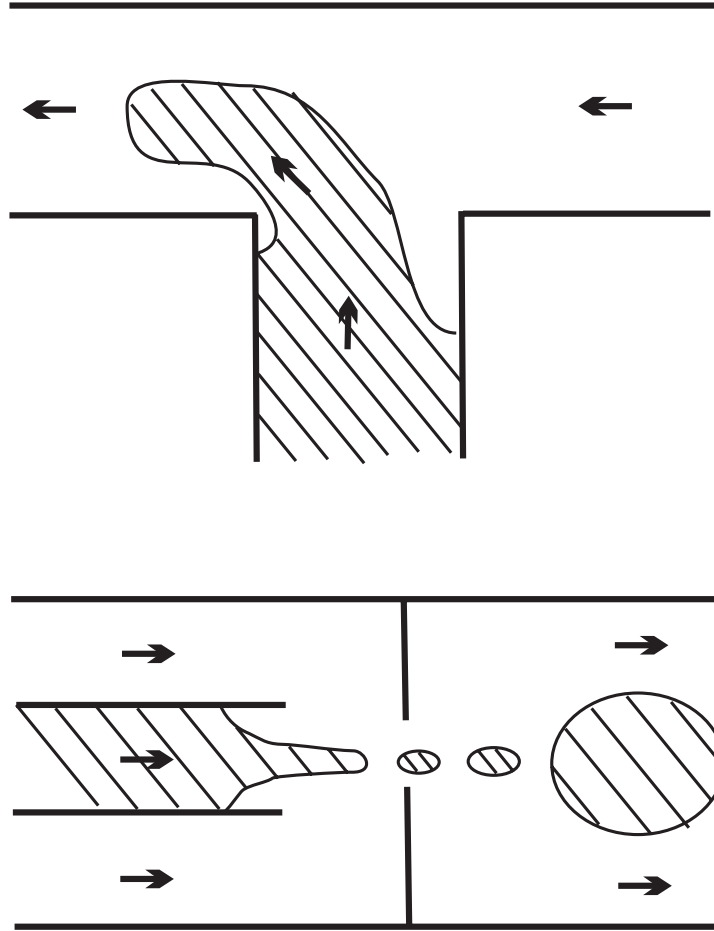


Figure 2: Some challenging free boundary problems involving moving contact lines between the oil (shaded) and water phases.

Tice et al. (2004) examined the influence of viscosity on the formation of droplets in microfluidic channels while Anna et al. (2003); Gañán Calvo and Gordillo (2001) showed how flow focussing (forcing a capillary jet through a narrow orifice) can lead to monodisperse formation of bubbles and droplets. Song et al. (2003) and Thorsen et al. (2001) examined microfluidic formation of droplets at T-junctions while Sugiura et al. (2001) and co-workers have experimented with different microfluidic geometries to develop monodisperse droplets.

### 3 Parameter estimation

A typical microfluidic channel in the network has a length of approximately  $L = 1$  cm and a width and height of around  $a = 100 \mu\text{m}$ . A typical flow rate of 1 ml/hr equates to a flow velocity in such a channel of the order of  $1 \text{ cm s}^{-1}$ . We take the dynamic and kinematic viscosities for water as  $\mu_w = 10^{-3} \text{ kg m}^{-1} \text{ s}^{-1}$  and  $\nu_w = 10^{-6} \text{ m}^2 \text{ s}^{-1}$ , respectively. The dynamic viscosity of oil is taken to be  $\mu_o = 10^{-2} \text{ kg m}^{-1} \text{ s}^{-1}$  and the surface tension at

the interface is assumed to be roughly  $\sigma \approx 50 \text{ dyn cm}^{-1}$ . From these values the Reynolds number and Capillary number are calculated to be

$$\text{Re} = \frac{U a}{\nu_w} \sim 1, \quad \text{Ca} = \frac{\mu_w U}{\sigma} \sim 10^{-2}.$$

Clearly, surface tension effects are very dominant and this leads to some very interesting, but difficult, free boundary problems at the nodes where the oil and water phases meet (figure 2). Due to the time constraints of the Study Group week, we decided not to tackle these problems directly, but instead to concentrate on developing a multiphase (nonlinear) generalisation of an electric-circuit theory model. This is described in the section below.

## 4 A network model

In this section we consider the flow in two model networks:

- A ‘Wheatstone bridge’ network, which has two inlets and two outlets, as illustrated in figure 3. This network has just 8 links and 8 nodes and has been studied experimentally by Unilever.
- A parallel mixing network, which has three inlets and  $m+1$  outlets for some positive number  $m$ , as shown in figure 4. This produces droplets from single phase inlet flows, and is an example of a possible application of the technology. The network has  $8m + 5$  links and  $6m + 6$  nodes. Water flows in through inlet node 2, whilst oil enters through inlet nodes 1 and 3. The idea is that oil droplets in water are formed at nodes 6, 11,  $\dots$ ,  $5m + 4$ , and that compound droplets of oil in water in oil form at nodes 8, 13,  $\dots$ ,  $5m + 5$ .

The volume flow rates of oil and water in each of the  $j = 1, 2, \dots, L$  links are  $q_{oj}$  and  $q_{wj}$  and the pressure at each of the  $i = 1, 2, \dots, N$  nodes is  $p_i$ . Note that we will assume that the pressure in each of the phases is equal. The effect of differing fluid pressures, due, for example, to surface tension, could be included in the model at a later date.

We describe the network using an  $N \times L$  matrix  $E$ . If the  $j$ th link connects the  $i_1$ th and  $i_2$ th nodes, with  $i_1 < i_2$ , then the  $j$ th column of  $E$  has just two nonzero entries,  $-1$  in the  $i_1$ th row and  $+1$  in the  $i_2$ th row. The matrix  $E$  is therefore sparse with just  $2L$  nonzero entries. We measure flow rates in each link to be positive in the direction from the  $i_1$ th to the  $i_2$ th node.

We will consider pressure-driven flows, which is more likely to be the arrangement used in practice, with pressures prescribed at the  $I$  inlet and  $O$  outlet nodes and the inlet and outlet flow rates to be determined.

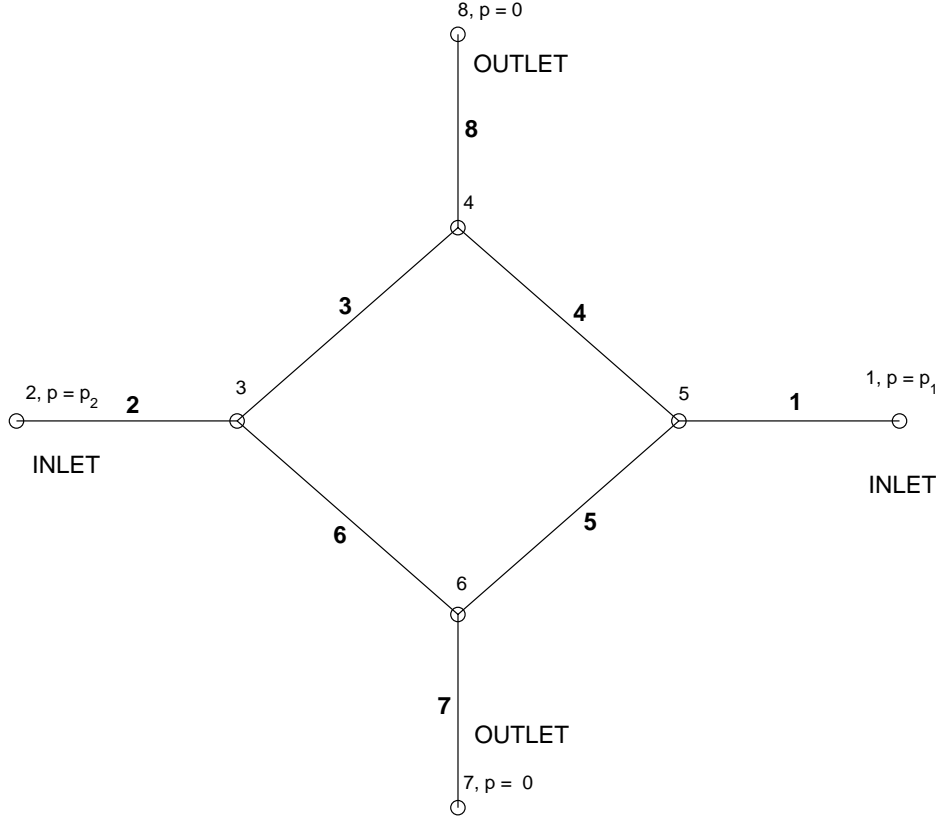


Figure 3: The Wheatstone bridge network. Bold face numbers refer to links and plain numbers to nodes in the network.

#### 4.1 Single phase flow

Conservation of mass gives

$$\sum_{j=1}^L E_{ij} q_{oj} \equiv E \mathbf{q}_o = 0, \quad (1)$$

where  $E_{ij}$  are the components of the matrix  $E$  and  $\mathbf{q}_o$  is a column vector with components  $q_{oj}$ .

If we assume that the flow in each of the links is laminar, the pressure drop across each link is linearly related to the flow rate by

$$p_{i_1} - p_{i_2} \equiv -\mathbf{p}E = \frac{k_j \mu_o L_j}{r_j^4} q_{oj}, \quad (2)$$

where  $\mathbf{p}$  is a row vector with components  $p_i$ ,  $\mu_o$  is the viscosity of the oil,  $L_j$  the length of the  $j$ th link,  $r_j$  a length representative of the cross-sectional length scale of the link and  $k_j$  a constant, dimensionless shape factor. For example, for laminar, Poiseuille flow in a pipe of circular cross-section,  $k_j = 8/\pi$ . We will assume that there is no pressure loss

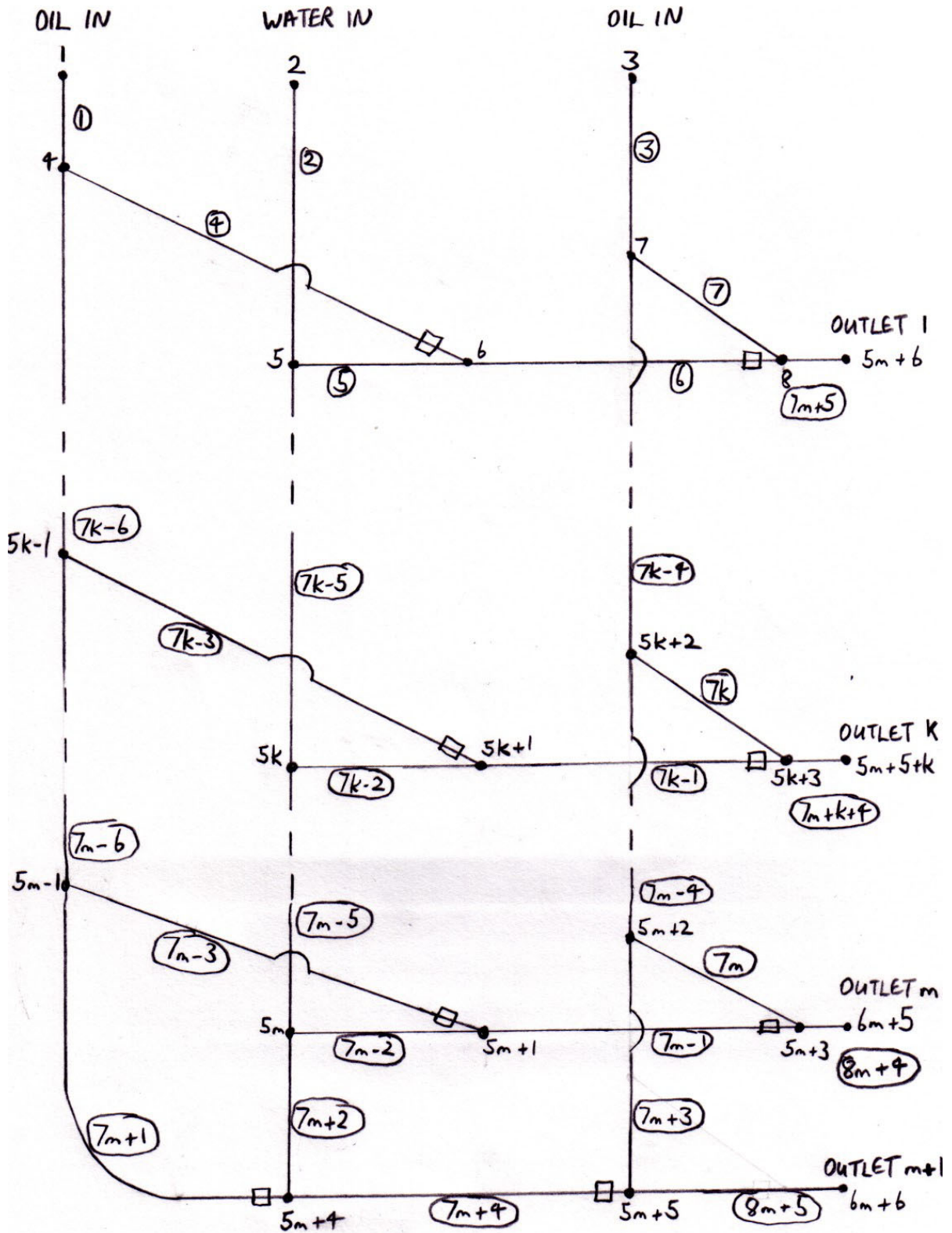


Figure 4: The parallel mixing network.

across the nodes, although this could be included in the model. Note that the matrix-vector multiplication form of (1) and (2) indicates that representing the network using the sparse matrix  $E$  is a sensible approach.

There are  $N - O - I$  unknown pressures and  $L$  unknown flow rates, whilst conservation of mass, (1), provides  $N - O - I$  equations, and the dynamical relation (2),  $L$  equations. Equations (1) and (2) therefore provide a linear system of  $N - O - I$  equations and  $N - O - I$  unknowns.

Rather than use the applied pressure as a basis for nondimensionalizing the system, we will use the capillary pressure  $p_c = 2\sigma/r$  due to a hemispherical oil/water meniscus of radius  $r$ , with  $r$  a typical cross-sectional channel dimension. The reasons for this will become clear in the next section. The flow rate due to this pressure drop in a channel of length  $L$  is  $q_c = 2\sigma r^3/k\mu_o L$ , where  $k$  is a typical shape factor. Typically,  $p_c \approx 1000\text{Pa}$  and  $q_c \approx 4 \times 10^{-10}\text{m}^3\text{s}^{-1}$ , in line with the typical values given in section 3. We therefore define dimensionless variables

$$\hat{p}_j = \frac{p_j}{p_c}, \quad \hat{q}_{oj} = \frac{q_{oj}}{q_c}, \quad (3)$$

in terms of which (1) and (2) become

$$\sum_{j=1}^L E_{ij} \hat{q}_{oj} \equiv E \hat{\mathbf{q}}_o = 0, \quad (4)$$

$$\hat{p}_{i_1} - \hat{p}_{i_2} \equiv -\hat{\mathbf{p}}E = R_j \hat{q}_{oj}, \quad (5)$$

where

$$R_j = \frac{k_j L_j r^4}{k L r_j^4} \quad (6)$$

is the resistance of the  $j$ th link. Equations (4) and (5) are equivalent to Kirchhoff's laws for an electrical network, with pressure difference equivalent to voltage difference, and flow rate equivalent to current. It is well known that the linear equations (4) and (5) subject to prescribed inlet and outlet pressures are linearly independent, and therefore have a unique solution.

Figure 5 shows a typical solution for the Wheatstone bridge network illustrated in figure 3, with unit resistance in each link, driven by unequal inlet pressures. We should also note that if one of the inlet pressures is too low, the flow may reverse and flow out through an inlet and possibly in through an outlet. For single phase flow, if we assume that the outlets are attached to oil reservoirs at zero nominal pressure, this remains an acceptable solution. The situation is different for oil/water flows, as we shall see.

## 4.2 Oil/water flow

If both oil and water flow into a network and mix, we are faced with all the usual problems associated with multiphase flow (see, for example, Drew and Passman, 1999). We need models for the forces that the two phases exert upon each other and upon the

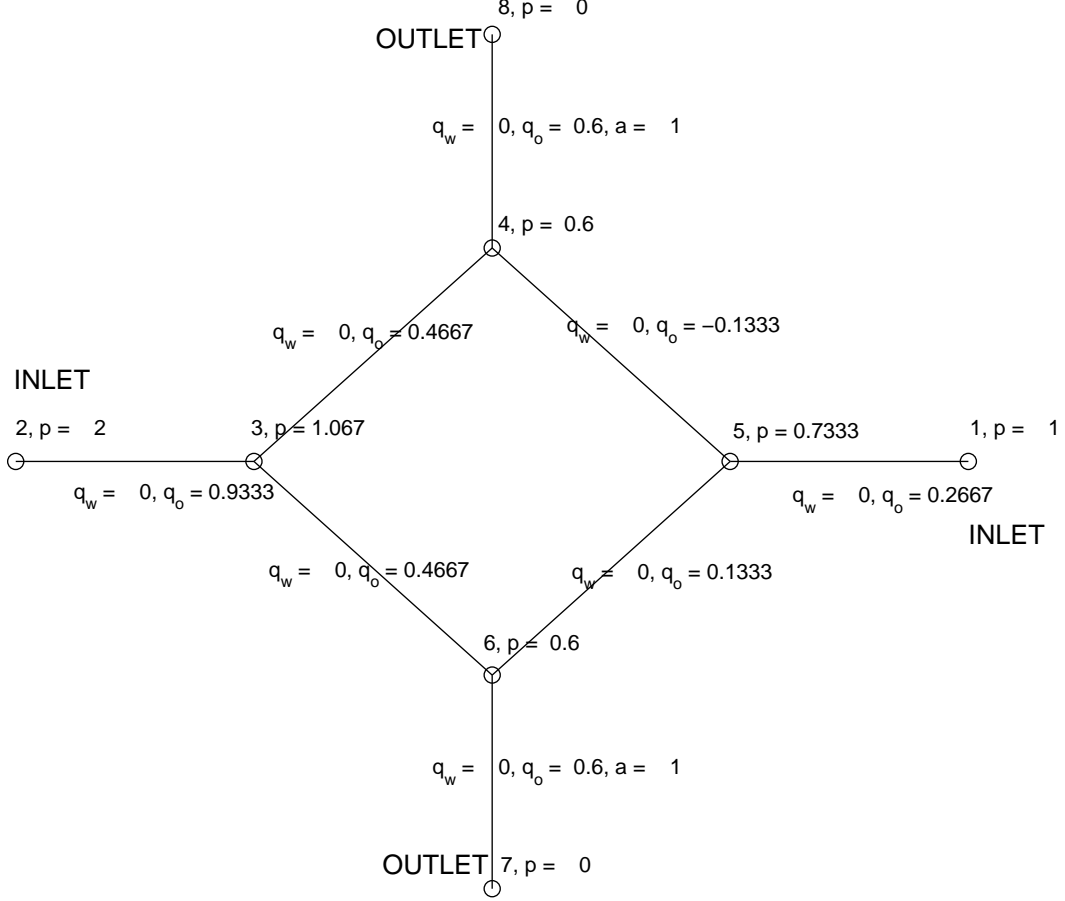


Figure 5: A typical solution for the flow of oil in the network shown in figure 3.

channel walls. For steady flow, this amounts to knowledge about the rate at which one fluid moves relative to the other, and the frictional pressure gradient in the channel. In the work reported here, we make the simplest possible assumption, which is that the fluids do not slip relative to each other, and that the frictional pressure gradient is linear in the two fluid flow rates. Irrespective of these considerations, conservation of mass at each node is given by

$$\sum_{j=1}^L E_{ij} \hat{q}_{oj} \equiv E \hat{\mathbf{q}}_o = 0, \quad \sum_{j=1}^L E_{ij} \hat{q}_{wj} \equiv E \hat{\mathbf{q}}_w = 0. \quad (7)$$

The linearity of the frictional pressure gradient can be expressed as

$$\hat{p}_{i_1} - \hat{p}_{i_2} \equiv -\hat{\mathbf{p}}E = R_j (\hat{q}_{oj} + \mu \hat{q}_{wj}), \quad (8)$$

where  $\mu = \mu_w / \mu_o \approx 0.1$ .

In pressure-driven flows, which we study here, we must also specify the pressure at  $I$  inlet and  $O$  outlet nodes, as we did for single phase flow. However, at the inlet nodes

we must also specify the composition of the incoming fluid to be either oil or water. There are  $N - O - I$  unknown pressures and  $2L$  unknown flow rates, whilst conservation of mass (7) provides  $2(N - O - I)$  equations, the dynamical relation (8)  $L$  equations, and knowledge of the inlet composition a further  $I$  equations. The number of unknowns therefore exceeds the number of equations by  $L - N + O$ . We can see where this imbalance comes from by considering a simple network with  $I$  inlets and  $O$  outlets joined at a single interior node. In this case  $N = I + O + 1$  and  $L = I + O$ , so that  $L - N + O = O - 1$ , and the number of extra equations required depends solely on the number of outlets. The extra equations are required to specify how the fluid phases divide as they leave the node. This conclusion applies in general to any internal node in a network. If the flow leaves a given node through  $n$  links, then  $n - 1$  extra equations must be applied at that node. There is a simple, and plausible, way of obtaining these extra equations. We calculate the total oil and water flow rates into the  $i$ th node,  $Q_{oi}$  and  $Q_{wi}$ , and deduce the mean inlet oil fraction,  $\alpha_i = Q_{oi}/(Q_{oi} + Q_{wi})$ . The new conditions are that the oil fraction should be  $\alpha_i$  in each of the links where the flow is directed out of the node. The key point is that once we have applied these equations in  $(n - 1)$  of the outflow links, applying it in the remaining outflow link is not necessary by conservation of mass (7). This means that these extra conditions, which we note are nonlinear, can be applied at each node in the network without having to determine a priori which nodes have more than one link with outflow. The “equal oil fraction” law agrees with the numerical experiments of Stark and Manga (2000). Some of the constraints associated with trying to apply different extra conditions are described later in section 6.

It was also felt that we should include the effect of an oil/water meniscus at junctions where drops are formed. The capillary pressure due to such a meniscus is around  $2\sigma/r_j$ , where  $\sigma$  is the surface tension. If the magnitude of the pressure drop across the link is less than this, no flow occurs. We can build this into the model by including an additional pressure loss in links where we know a priori that the fluid is exiting into a single phase flow of the fluid that does not form the continuous phase. We rewrite (8) as

$$\begin{aligned} \hat{p}_{i_1} - \hat{p}_{i_2} \equiv -\hat{\mathbf{p}}E = R_j (\hat{q}_{oj} + \mu\hat{q}_{wj}) + C \operatorname{sgn}(\hat{q}_{oj} + \hat{q}_{wj}) & \quad \text{for} \quad |\hat{q}_{oj} + \hat{q}_{wj}| > 0, \\ |\hat{p}_{i_1} - \hat{p}_{i_2}| \leq C & \quad \text{for} \quad \hat{q}_{oj} + \hat{q}_{wj} = 0. \end{aligned} \quad (9)$$

Since we have nondimensionalized pressure on a capillary scale, we expect that  $C$  is  $O(1)$ , and in the following results, we have taken  $C = 1$  when using this modified flow law. In fact, we need to smooth out this discontinuous function to be able to use it in a numerical solver. We used

$$\hat{p}_{i_1} - \hat{p}_{i_2} = R_j (\hat{q}_{oj} + \mu\hat{q}_{wj}) + C \operatorname{sgn}(\hat{q}_{oj} + \hat{q}_{wj}) (1 - e^{-|\hat{q}_{oj} + \hat{q}_{wj}|/q_{sm}}), \quad (10)$$

with  $q_{sm} = 10^{-4}$ . There are other possibilities that could be used as dynamic laws instead of (10), which are discussed in section 6.

In order to solve the nonlinear system of equations (7) and (10), along with specified inlet and outlet pressures and inlet oil fractions (0 or 1), we used Newton iteration, implemented as a MATLAB function. The version of the code that solves for the parallel mixing network is fully annotated, and listed as appendix A. It should be noted that the

code could be made much more efficient by reusing the Jacobian to give a quasi-Newton method, but we have not pursued this here. Even for a parallel mixing network with  $m = 100$ , the largest system tackled here, the solution can be obtained in about 15 minutes on a 2.8GHz Pentium IV PC.

Before presenting some results, we should note that for both types of network, whether or not the effect of oil/water menisci was included, we found no numerical evidence for non-uniqueness of the solution. When we started by finding the solution for either single phase oil, single phase water or an oil fraction of 0.5 in each inlet, and then used this as the initial guess for the situations described below, the solution to which the iteration converged was always the same. We have not, however, attempted to *prove* that the solution is unique, although this is an interesting problem.

### 4.3 Results for the Wheatstone bridge network

In figure 6 we show the solution when single phase oil enters through node 1 and single phase water through node 2. Mixing therefore occurs at nodes 4 and 6, but, to begin with, we have not included the effect of the oil/water meniscus in links 4 and 5 (see figure 3). In figure 6a, the outlet oil fraction is about 0.22 at node 7 and also, by symmetry, at node 8. If we reduce the pressure at the water inlet, the water flow rate decreases, as we would expect, until, when  $p \approx 2.5$ , the water flow rate falls to zero. Only oil then flows through the network, as shown in figure 6b. If we drop the water inlet pressure further, node 2 becomes an outlet for single phase oil.

Figure 7 shows the analogous results when we include the effect of the oil/water meniscus in links 4 and 5. As we would expect, the pressure losses across these links are higher than those shown in figure 6, and the water inlet pressure can fall slightly more before the flow rate of water falls to zero.

### 4.4 Results for the parallel mixing network

Figures 8 to 10 show the outlet flow rates and outlet oil fractions for parallel mixing networks of various sizes. The effect of the oil/water meniscus in the appropriate links (see figure 4) has been included. In addition, the inlet flow lines for the single phase oil and water (links  $7k - 6$ ,  $7k - 5$  and  $7k - 4$  for  $k = 1, 2, \dots, m$  and  $7m + 1$ ,  $7m + 2$  and  $7m + 3$  in figure 4) have resistances 100 times smaller than that of each of the links within the network. The reasons for this are discussed in section 5. In each network, the flow rates decrease the further the outlet is from the inlet, as the driving pressure is decreased by the frictional pressure drop. In addition, the outlet oil fractions decrease along the network, since the oil outlet flow rates fall more rapidly than the water outlet flow rates, as a consequence of the higher viscosity of the oil. As the number of outlets increases, the outlet conditions appear to converge towards a form that is independent of the number of outlets. This phenomenon could be investigated using an asymptotic approach valid for large  $m$ , which could take the form of an effective medium theory, but

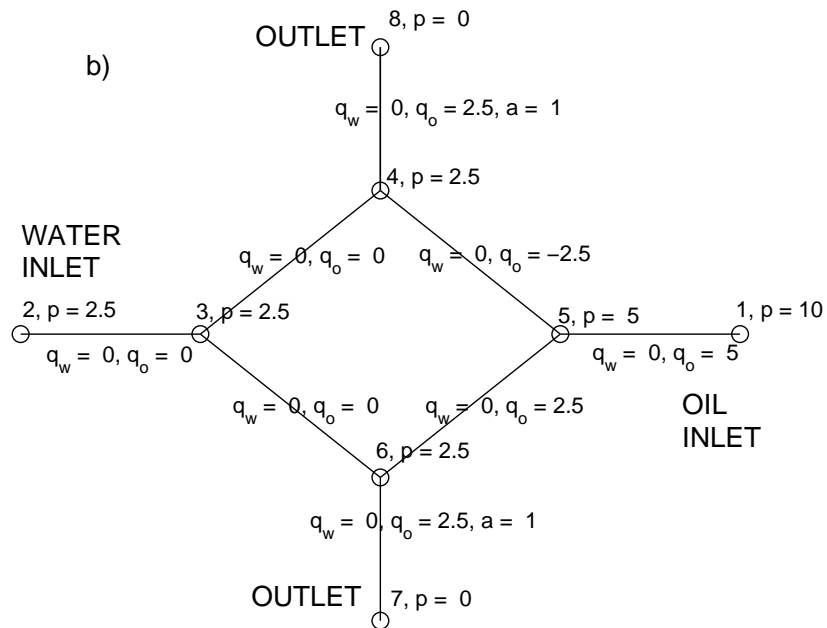
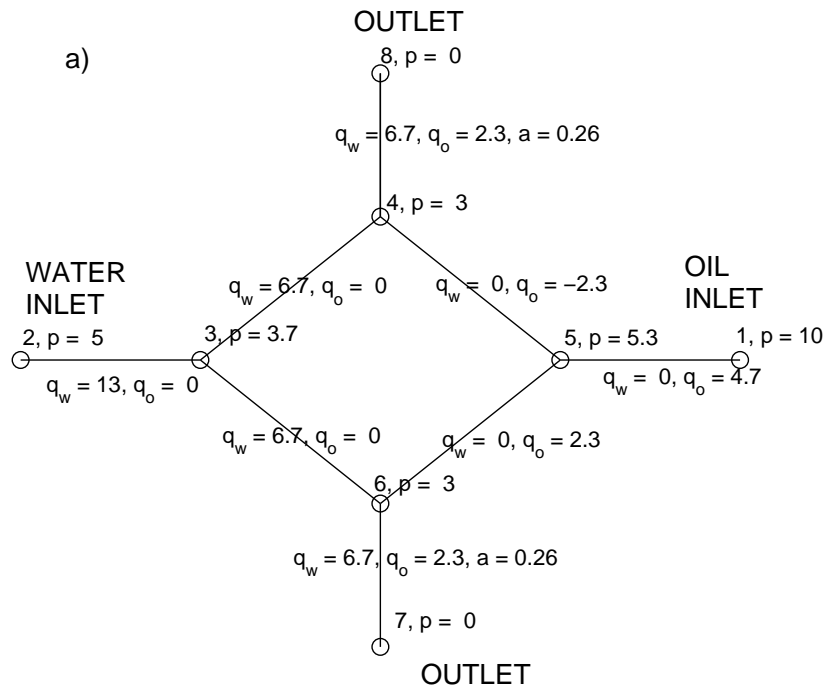


Figure 6: Two solutions for the flow of oil and water in the network shown in figure 3. In b), the inlet water pressure is too low to drive any flow, and single phase oil leaves the outlet. If  $p_2 < 2.5$ , single phase oil would also be driven out of inlet node 2.

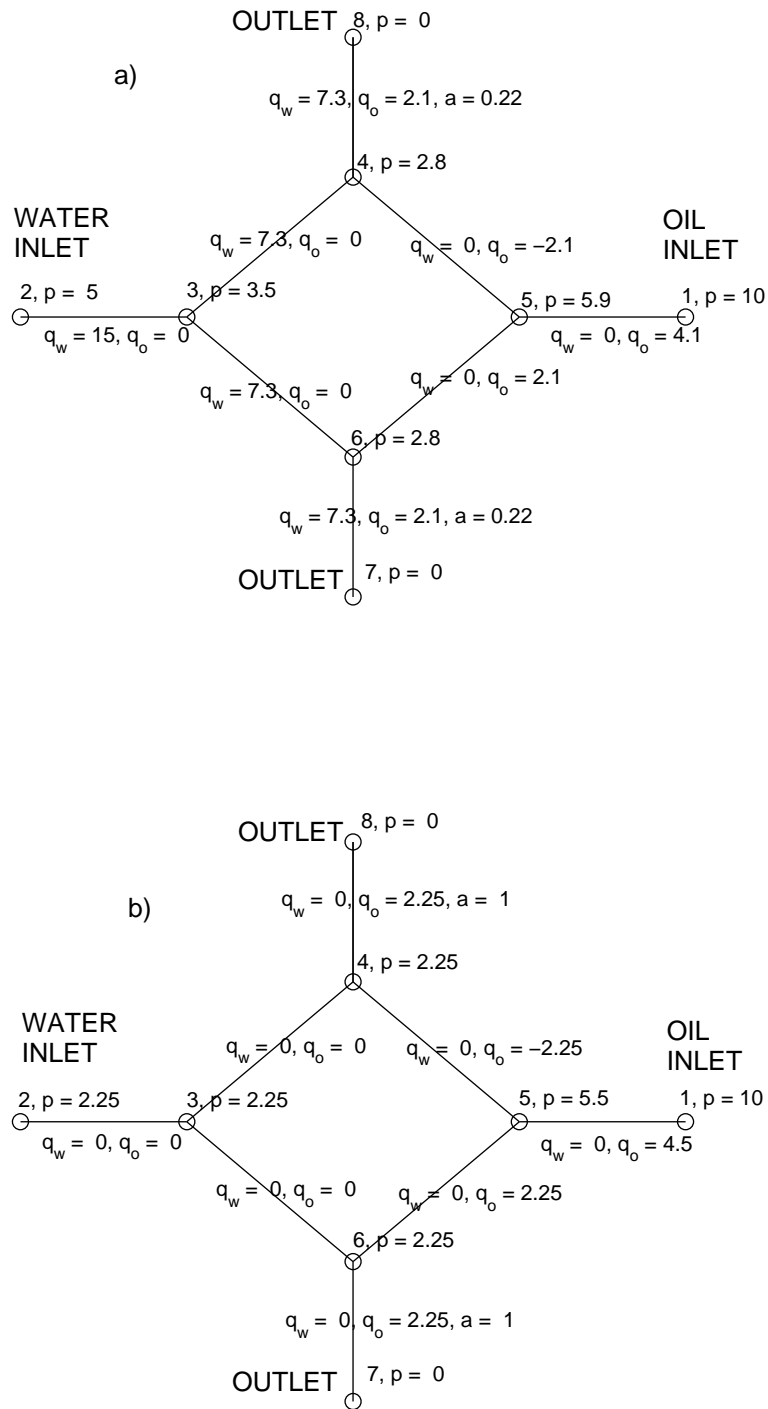


Figure 7: Two solutions for the flow of oil and water in the network shown in figure 3, including the effect of an oil/water meniscus in links 4 and 5. In b), the inlet water pressure is too low to drive any flow, and single phase oil leaves the outlet. If  $p_2 < 2.25$ , single phase oil would also be driven out of inlet node 2.

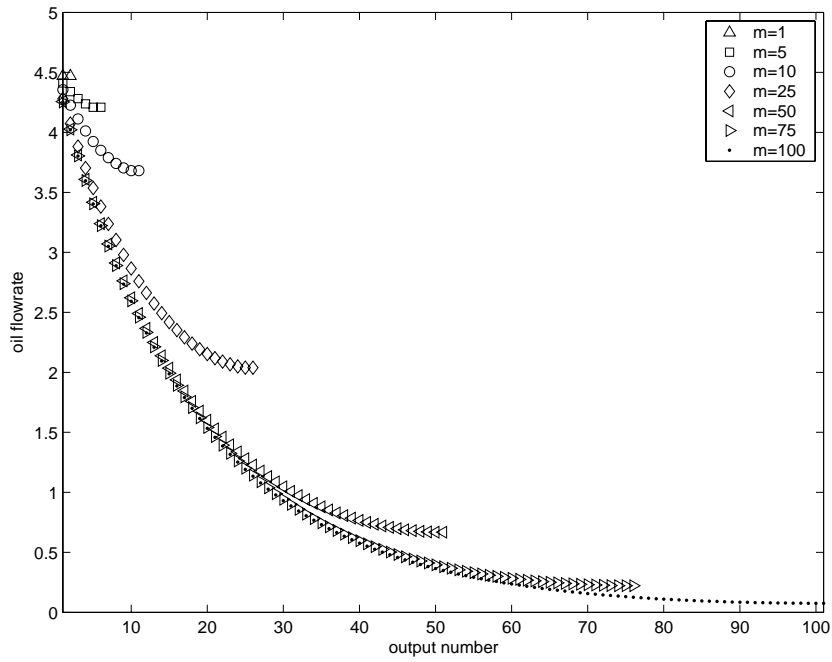


Figure 8: The outlet oil flow rates for parallel mixing networks of various sizes. All inlet pressures are equal to 10.

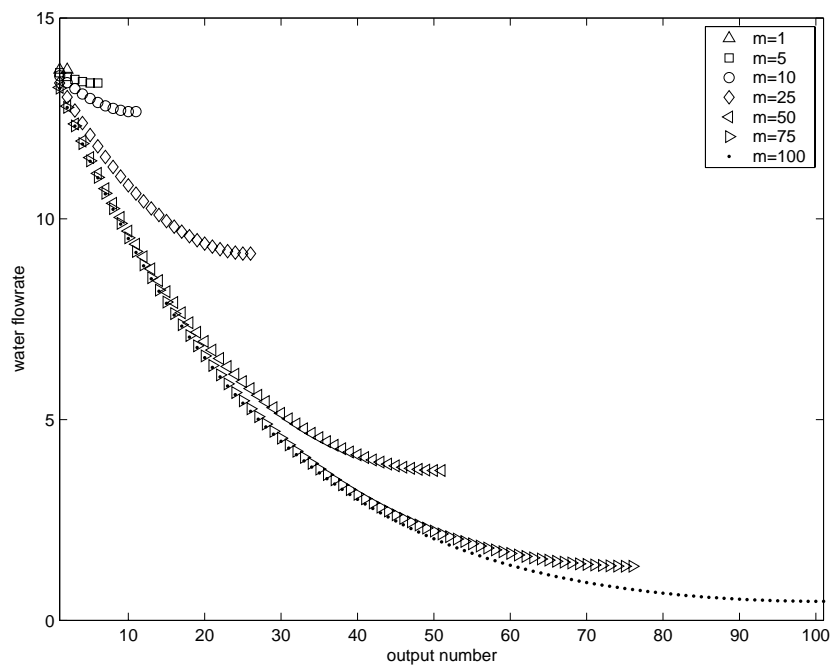


Figure 9: The outlet water flow rates for parallel mixing networks of various sizes. All inlet pressures are equal to 10.

we have not investigated this further here. We also found that if the inlet pressure was too low, it was not sufficient to drive a flow through the network, as we would expect.

The outlet oil flow rates can be increased by increasing the pressure at the oil inlets. However, for sufficiently high oil inlet pressures, the water is unable to hold back the oil, which flows into the water inlet line through link 5 (see figure 4). This is illustrated in figure 11. Once the inlet pressure at node 2 increases past 13.98, oil flows through node 5. Of course, in this case there is now no longer an oil/water meniscus in link 4, but there is in link 5.

## 5 Stability of parallel microfluidic networks

As mentioned in the introduction, it may be necessary to operate many microfluidic devices simultaneously, for example in order to obtain a high production rate of droplets; or to test for the presence of many different chemicals at one time. Instead of utilising a large number of self-contained microfluidic circuits, the component devices may be connected *in parallel*, as shown in figures 4 and 12.

Microfluidic devices connected in parallel share a single fluid supply pump and other supporting infrastructure. This greatly reduces the overall cost and physical complexity of the system. However, the user can only control the behaviour of the network by adjusting the fluid flow rate at the inlet,  $Q_{\text{in}}$ , and the pressure at the outlet,  $p_{\text{out}}$ . It is important that each branch of the network should operate reliably with this low level of control, even if the exact pressure-flow characteristics of the individual branches in the network differ due to variations during the manufacture of the network. Therefore in the following sections we consider how network design and device manufacturing tolerances affect the performance of a massively parallel microfluidic network, and show how the stability of networks can be improved.

### 5.1 A parallel array of nozzles

We will analyse a parallel array of nozzles shown in figure 12. This circuit could be used for a simple droplet production process. The network is made up of  $N$  parallel branches which are fed with fluid from a single low-resistance supply vessel, and drain into a single large output vessel. Each branch contains a single nozzle, connected to the main fluid supply vessel by a channel with resistance  $R_i$ , as described by equation (5). The pressure-flow characteristics of the nozzles are represented by nonlinear resistances. The pressure drop across the  $i$ th nozzle,  $\Delta p_i^{(f)}$ , is related to the flux of fluid in the nozzle,  $q_i$ , by the expression

$$\Delta p_i^{(f)} = f_i(q_i) \quad \text{for } i = 1, 2, \dots, N.$$

We now account for the small variations in the flow characteristics of the channels and nozzles which result from the manufacturing process. We express the resistances  $R_i$  and the functions  $f_i(q)$  as the sum of the average values,  $\bar{R}$  and  $\bar{f}(q)$  respectively, which are

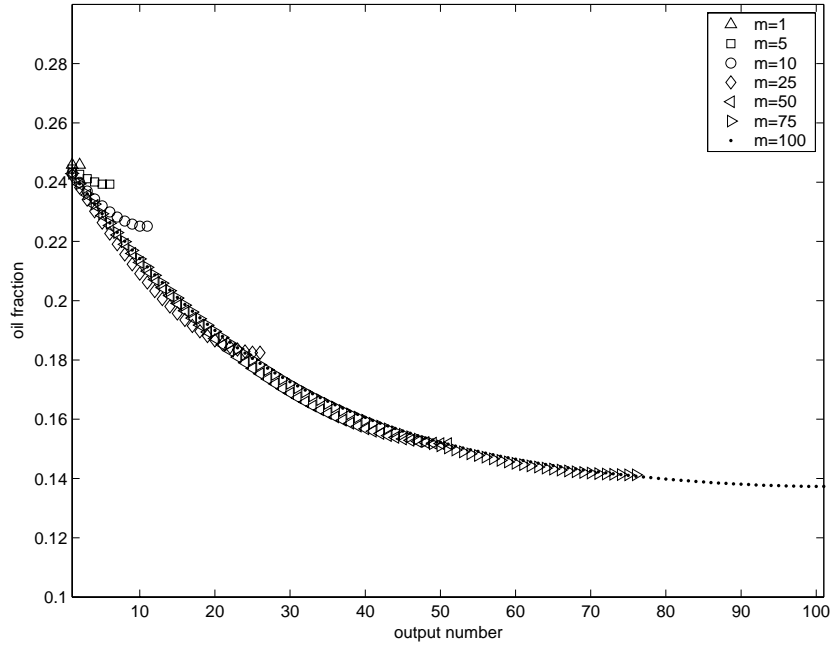


Figure 10: The outlet oil fractions for parallel mixing networks of various sizes. All inlet pressures are equal to 10.

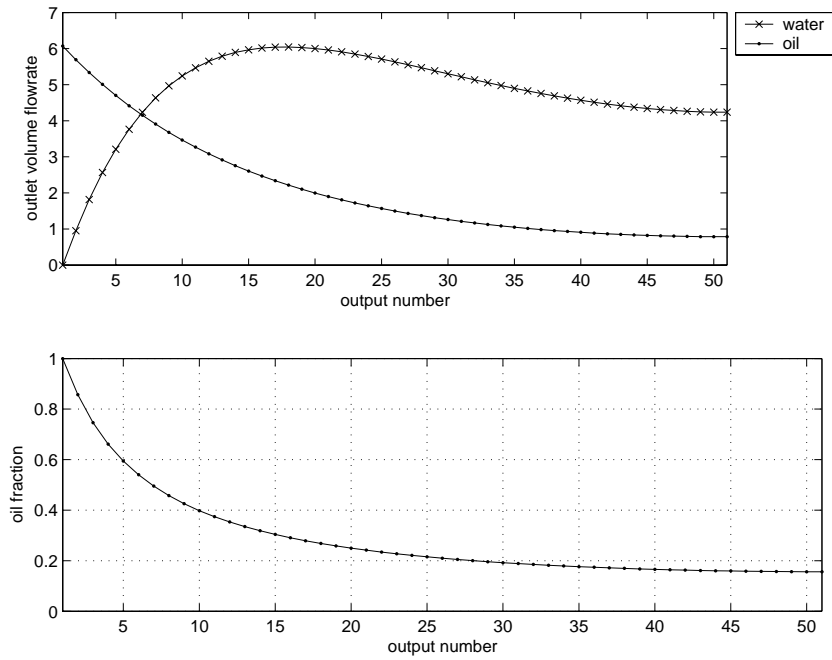


Figure 11: The outlet flow rates and outlet oil fractions for a parallel mixing network with  $m = 50$ . The water inlet pressure is 10, as is the oil inlet pressure at node 3, whilst the oil inlet pressure at node 2 is 13.98. For higher pressures at node 2, oil enters the water inlet flow line through node 5.

independent of  $i$ , and a small correction term which represents the variations between the components:

$$R_i = \bar{R} + \epsilon \hat{R}_i, \quad f_i(q) = \bar{f}(q) + \epsilon \hat{f}_i(q) \quad \text{for } i = 1, 2, \dots, N, \quad (11)$$

where  $0 < \epsilon \ll 1$  is a measure of the manufacturing tolerance, and

$$\bar{R} = \frac{1}{N} \sum_{i=1}^N R_i, \quad \bar{f}(q) = \frac{1}{N} \sum_{i=1}^N f_i(q) \quad \text{for all } q.$$

Note that the definitions of  $\hat{R}_i$  and  $\hat{f}_i$  imply that

$$\sum_{i=1}^N \hat{R}_i = 0, \quad \sum_{i=1}^N \hat{f}_i(q) = 0 \quad \text{for all } q.$$

The mathematical description of the system is straightforward. Conservation of mass in the network requires

$$Q_{\text{in}} = \sum_{i=1}^N q_i. \quad (12)$$

Because the input and output vessels are assumed to have a very low resistance to flow, the total pressure drop across each branch of the network is equal to the difference of the inlet and outlet pressures. Therefore

$$p_{\text{in}} - p_{\text{out}} = R_i q_i + f_i(q_i) \quad \text{for } i = 1, 2, \dots, N. \quad (13)$$

We seek a solution of (11)–(13), to determine the  $q_i$  and  $p_{\text{in}}$ , using regular perturbation analysis. We expand the fluxes,  $q_i$ , and the inlet pressure in powers of  $\epsilon$ :

$$q_i = q_i^{(0)} + \epsilon q_i^{(1)} + \epsilon^2 q_i^{(2)} + \dots \quad (14)$$

$$p_{\text{in}} = p_{\text{in}}^{(0)} + \epsilon p_{\text{in}}^{(1)} + \epsilon^2 p_{\text{in}}^{(2)} + \dots \quad (15)$$

Substituting these expansions into (11)–(13) and collecting the leading order terms, we find

$$Q_{\text{in}} = \sum_{i=1}^N q_i^{(0)}, \quad (16)$$

$$p_{\text{in}}^{(0)} - p_{\text{out}} = \bar{R} q_i^{(0)} + \bar{f}(q_i^{(0)}). \quad (17)$$

The leading order problem is solved by an even distribution of the fluxes between the branches,

$$q_i^{(0)} = \frac{Q_{\text{in}}}{N}, \quad p_{\text{in}}^{(0)} = \frac{\bar{R} Q_{\text{in}}}{N} + \bar{f}(Q_{\text{in}}/N). \quad (18)$$

At the next order,  $\mathcal{O}(\epsilon)$ , the perturbations  $\hat{R}_i$  and  $f_i(q)$  enter the analysis. Equations for  $q_i^{(1)}$  and  $p_{\text{in}}^{(1)}$  are found by inserting the expansions (14) and (15) into equations (11)–(13) and retaining terms of  $\mathcal{O}(\epsilon)$  only. We find

$$0 = \sum_{i=1}^N q_i^{(1)}, \quad (19)$$

$$p_{\text{in}}^{(1)} = \bar{R} q_i^{(1)} + \hat{R}_i q_i^{(0)} + \hat{f}_i(q_i^{(0)}) + q_i^{(1)} \left( \frac{df}{dq} \right) \Big|_{q=q_i^{(0)}}. \quad (20)$$

Solving equations (19) and (20), we obtain

$$q_i^{(1)} = - \frac{\hat{R}_i Q_{\text{in}}/N + \hat{f}_i(Q_{\text{in}}/N)}{\bar{R} + \left( \frac{df}{dq} \right) \Big|_{q=(Q_{\text{in}}/N)}}, \quad p_{\text{in}}^{(1)} = 0. \quad (21)$$

Combining the leading order solution, (18), and the first correction, (21), we have shown that the flux in the  $i$ th branch of the network is described by

$$q_i = \frac{Q_{\text{in}}}{N} - \epsilon \frac{\hat{R}_i Q_{\text{in}}/N + \hat{f}_i(Q_{\text{in}}/N)}{\bar{R} + \left( \frac{df}{dq} \right) \Big|_{q=(Q_{\text{in}}/N)}} + \dots, \quad (22)$$

$$= \frac{Q_{\text{in}}}{N} - \frac{(R_i - \bar{R}) Q_{\text{in}}/N + (f_i(Q_{\text{in}}/N) - \bar{f}(Q_{\text{in}}/N))}{\bar{R} + \left( \frac{df}{dq} \right) \Big|_{q=(Q_{\text{in}}/N)}} + \dots \quad (23)$$

Equation (23) shows that the differences between the fluxes in the  $i$ th branch and the average flux  $\bar{q} = Q_{\text{in}}/N$  depends on  $(R_i - \bar{R})$  and  $(f_i(q) - \bar{f}(q))$ , as expected. However, (23) also shows  $(q_i - \bar{q})$  may be reduced by making the average channel resistance,  $\bar{R}$ , large. This occurs because the fluid flow divides between the branches according to the *overall* flow resistance of the branch. By increasing  $\bar{R}$ , the deviations in the resistance of the channels and nozzles become small compared to the overall resistance of the branch, and their effect on the division of the flow will be also small. However, it may only be possible to increase the mean resistance  $\bar{R}$  of the vessels whilst keeping errors  $\hat{R}_i$  of the same order of magnitude by *lengthening* the channel (not by narrowing). Such a requirement of long input channels may create some difficulties in compact device design.

We can also consider the effect on the network operation of blocking some branches of a parallel network. If a proportion  $p$  ( $0 \leq p \leq 1$ ) of the channels become blocked, the change in the flux per channel will be

$$\Delta \bar{q} = \frac{Q_{\text{in}}}{N} - \frac{Q_{\text{in}}}{N - pN} \quad (24)$$

$$= \frac{Q_{\text{in}}}{N} \left( \frac{p}{1 - p} \right). \quad (25)$$

Thus the change in the average flux per channel due to channel-blocking events decreases as  $N \rightarrow \infty$ . Therefore channel blocking will cause less disruption to the operating regime of the remaining open channels if  $N$  is large.

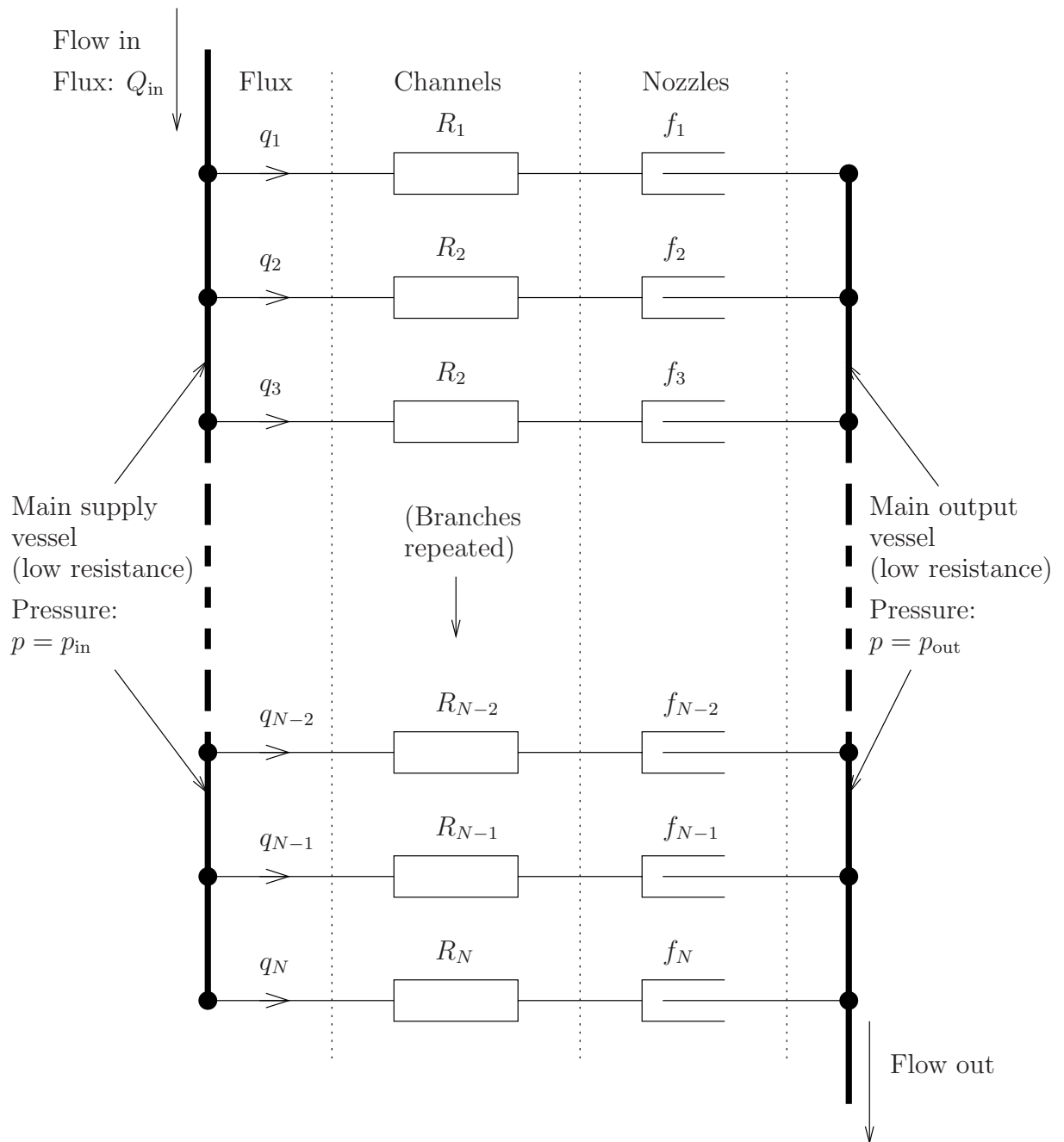


Figure 12: The parallel array of nozzles, analysed in Section 5.1.

## 6 Further comments

### 6.1 Imposing other nodal conditions

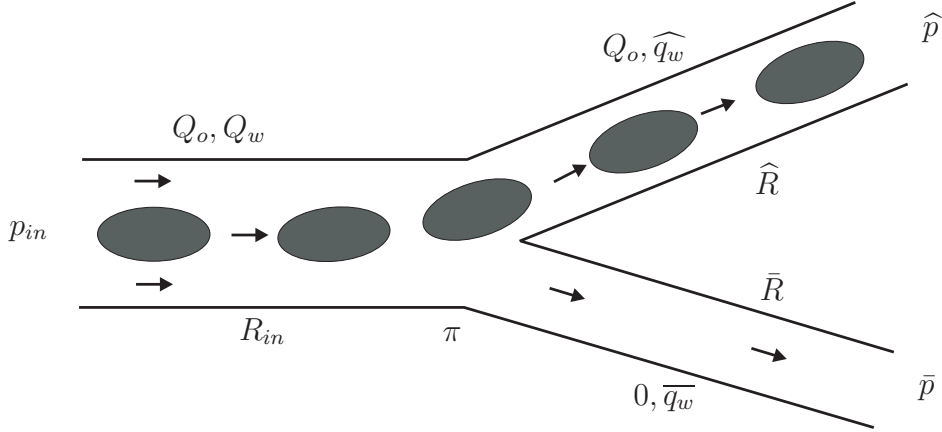


Figure 13: Imposing other nodal laws: the case when all oil droplets enter the same preferential outgoing channel.

In the derivation of our two-phase network model in section 4.2, extra conditions were required at nodes where flow splitting occurs, to specify how the phases divide as they leave the node. For the subsequent calculations, the simple condition of equal oil/water fraction into each outgoing channel was used. However, the work of Manga (1996) reveals that the equal oil/water fraction is an oversimplification of the droplet dynamics at a bifurcation. Indeed, droplet size and structure, viscosity ratio, capillary number as well as the network vessel properties themselves all have the ability to alter the proportion of droplets entering a particular outgoing channel at a junction.

A natural question to now ask is: can other nodal conditions be imposed in our network model? To test such an idea, we examine whether a nodal law for which every oil droplet is drawn down a single outgoing channel will lead to a consistent set of equations. For simplicity, we take a single bifurcating node (figure 13) where the incoming flow is a mixed phase of oil droplets and water. The upstream and downstream pressures  $p_{in}$ ,  $\hat{p}$  and  $\bar{p}$  are set. The incoming oil and water volume flow rates are  $Q_o$  and  $Q_w$  respectively and the ratio of the two is fixed. Without loss of generality, we assume the pressure drop into the upper branch ( $p_{in} - \hat{p}$ ) is larger than the pressure drop into the lower branch ( $p_{in} - \bar{p}$ ) and that **all** the oil droplets are thus drawn into the upper branch (our new nodal condition). The resistances of the upstream mother vessel  $R_{in}$ , the upper outgoing vessel  $\hat{R}$  and the lower outgoing vessel  $\bar{R}$  are known and the water phase splits into volume flow rates  $\hat{q}_w$  and  $\bar{q}_w$  in the upper and lower outgoing vessels respectively.

From the model in section 4, the following system of equations arises:

$$(p_{in} - \pi) = R_{in}(\mu Q_w + Q_o), \quad (26)$$

$$(\pi - \hat{p}) = \hat{R}(\mu \hat{q}_w + Q_o), \quad (27)$$

$$(\pi - \bar{p}) = \bar{R}\mu \bar{q}_w, \quad (28)$$

$$Q_w = \hat{q}_w + \bar{q}_w, \quad (29)$$

where  $\pi$  is the internal pressure at the node itself. The first equation (26) is only required to determine the magnitude of the incoming volume flow rates; any possible constraint can be found from the other equations. Eliminating  $\pi$  from (27) and (28) and solving for the water volume flow rate  $\bar{q}_w$  in the lower vessel, using (29), leads to

$$\bar{q}_w = \frac{\hat{R}}{\mu(\hat{R} + \bar{R})} \left( \mu Q_w + Q_o - \frac{(\bar{p} - \hat{p})}{\hat{R}} \right).$$

This solution is only physically sensible if the water volume flow rate into the lower outgoing channel is less than the incoming water volume flow rate,  $\bar{q}_w \leq Q_w$ . Otherwise, water would have to be drawn in from the upper channel, leading to the water and oil phases travelling in opposite directions there. Of course,  $\bar{q}_w < 0$  is perfectly acceptable, resulting in the lower outgoing channel feeding water into the mixed phase upper channel,  $\hat{q}_w > Q_w$  (so long as the lower outgoing channel is connected to a water reservoir). Applying the inequality to the expression above leads to the constraint

$$\frac{\hat{R}}{\mu \bar{R}} \left( Q_o - \frac{(\bar{p} - \hat{p})}{\hat{R}} \right) \leq Q_w.$$

This constraint only allows oil droplets to all take the same channel out of the node if

- the pressure drop in the oil-laden channel is large enough compared to other outgoing channel (possibly reversing the flow in the other outgoing channel for instance);
- the resistance in the oil-laden channel ( $\hat{R}$ ) is much lower than the other outgoing channel;
- the viscosity ratio  $\mu$  is close to unity;
- the oil fraction is not too large ( $Q_o < \mu Q_w$  appears to be a reasonable rule-of-thumb).

Whilst we have approached the nodal condition and necessary constraint from a network point-of-view, it is worth noting that some of these observations above are similar to those made by Manga (1996) in terms of droplet dynamics and channel selection.

## 6.2 Alternative laws for the flow dynamics in the channels

Our network model is presently based on no-slip between the two phases, leading to a linear relationship between pressure and volume flux through a vessel. For single-phase carrying vessels this relationship is perfectly valid, but for mixed-phase channel flow large slip forces and nonlinear pressure-flux relationships must be considered. One example is that of Bretherton (1961), which applies to long bubbles (of volume exceeding  $4\pi r^3/3$  where  $r$  is the cross-sectional radius of the vessel itself) where the viscosity of the bubble can be neglected. In this case, the pressure-flux relation resembles (Stark and Manga, 2000)

$$Q \sim \Delta P - \sum_{\text{bubbles}} \Delta P_b(Q),$$

where  $Q$  is the mass flux,  $\Delta P$  is the pressure drop across the vessel and  $\Delta P_b$  is the pressure drop across each bubble, which is proportional  $\text{Ca}^{2/3}$ . In fact, the work of Wong et al. (1995b) in polygonal capillary channels suggests in certain regimes the pressure-flux relation  $\Delta P \sim Q^{2/3}$ . Future extensions to the network model could accommodate this behaviour depending on the oil fraction, capillary number, *etc.* However, it is important to note that these analyses may predict well the behaviour of gaseous bubbles inside a liquid phase, but not oil droplets, as their internal viscosity is likely to have a significant effect (see Hodges et al., 2004, for details).

## 7 Conclusions

By assuming no-slip between the two-phases, Kirchhoff's laws, which form the basis of electric-circuit theory, can be generalised to model two-phase flow in a microfluidic network of channels. For a network of  $N$  nodes and  $L$  links (channels), of which  $I$  nodes are inputs with pressure and phase composition specified and  $O$  are output nodes with pressure specified,  $L - N + O$  extra equations are required to explain how the phases divide at nodes. These equations must remain consistent with mass conservation of each phase, possibly leading to constraints. The simplest consistent condition to impose at the dividing nodes is that the volume fraction of each phase remains equal in each of the outgoing channels. For  $n$ -phase flow, it is straightforward to extend this network theory, imposing only one momentum equation in each channel, leading to  $(n - 1)(L - N + O)$  extra equations being needed. As with two-phase flow, imposing an equal volume fraction in each of the outgoing channels for each phase leads to a complete system consistent with mass conservation of each phase (proof by induction). Preliminary results for a Wheatstone bridge and parallel-mixing network have been obtained, although no non-uniqueness in the flow field has been found.

On the issue of network stability, we have shown that by making the overall resistance of the branches of a parallel network of microfluidic devices large relative to the expected variation of resistance between the branches, the division of the fluid flow across the network will become more uniform. This will allow consistent operation of the nozzles (or other components) in all branches of the network. Due to manufacturing tolerances,

however, this may only be possible by building long feeding channels, which will prove difficult to fit on to a compact device. We have also shown that large parallel networks are more resilient than small networks to blockages of some network branches. Overall, our work suggests that large parallel networks offer good prospects for boosting the efficiency and reliability of microfluidic circuits.

Microfluidics is clearly an important and growing area of research with many exciting questions to be answered. At present, we have only had time to examine steady network flow. The possibilities to look at unsteady drop formation at nodal junctions and the associated pressure rises and falls over time, which generate feedback through the system, appear some of the exciting challenges for the future.

## 8 Acknowledgements

We would like to thank John Melrose and Guoping Lian for bringing such an interesting problem to the Study Group. Many thanks are also due to the organisers for making the Study Group week such a highly enjoyable and successful event.

## References

- S. L. Anna, N. Bontoux, and H. A. Stone. Formation of dispersions using flow focussing in microchannels. *Appl. Phys. Lett.*, 82:364–366, 2003.
- A. Borhan and C. F. Mao. Effect of surfactants on the motion of drops through circular tubes. *Phys. Fluids A - Fluid Dynamics*, 4:2628–2640, 1992.
- A. Borhan and J. Pallinti. Breakup of drops and bubbles translating through circular capillaries. *Phys. Fluids*, 11:2846–2855, 1999.
- F. P. Bretherton. The motion of long bubbles in tubes. *J. Fluid Mech.*, 10:166–188, 1961.
- D. A. Drew and S. L. Passman. *Theory of multicomponent fluids*. Applied Mathematical Sciences. Springer-Verlag, 1999.
- A. M. Gañán Calvo and J. M. Gordillo. Perfectly monodisperse microbubbling by capillary flow focussing. *Phys. Rev. Lett.*, 87:274501, 2001.
- A. L. Hazel and M. Heil. The steady propagation of a semi-infinite bubble into a tube of elliptical or rectangular cross-section. *J. Fluid Mech.*, 470:91–114, 2002.
- S. R. Hodges, O. E. Jensen, and J. M. Rallison. The motion of a viscous drop through a cylindrical tube. *J. Fluid Mech.*, 501:279–301, 2004.
- M. Manga. Dynamics of drops in branched tubes. *J. Fluid Mech.*, 315:105–117, 1996.

- W. L. Olbricht. Pore-scale prototypes of multiphase flow in porous media. *Ann. Rev. Fluid Mech.*, 292:71–94, 1995.
- W. L. Olbricht and D. M. Kung. The deformation and breakup of liquid-drops in low Reynolds number flow through a capillary. *Phys. Fluids A - Fluid Dynamics*, 4:1347–1254, 1992.
- J. Ouellette. A new wave of microfluidic devices. *The Industrial Physicist*, 9(4):14–17, 2004.
- A. C. Payatakes. Dynamics of oil ganglia during immiscible displacement in water-wet porous-media. *Ann. Rev. Fluid Mech.*, 14:365–393, 1982.
- H. Song, J. D. Tice, and R. Ismagilov. A microfluidic system for controlling reaction networks in time. *Angew. Chem. Int. Ed.*, 42:768–772, 2003.
- J. Stark and M. Manga. The motion of bubbles in a network of tubes. *Transport in Porous Media*, 40:210–218, 2000.
- H. A. Stone, A. D. Stroock, and A. Ajdari. Engineering flows in small devices: Microfluidics toward a lab-on-a-chip. *Ann. Rev. Fluid Mech.*, 36:381–411, 2004.
- S. Sugiura, M. Nakajima, and M. Seki. Interfacial tension driven monodispersed droplet formation from microfabricated channel array. *Langmuir*, 17:5562–5566, 2001.
- T. Thorsen, R. W. Roberts, F. H. Arnold, and S. R. Quake. Dynamic pattern formation in a vesicle-generating microfluidic device. *Phys. Rev. Lett.*, 86:4136–4166, 2001.
- J. D. Tice, A. D. Lyon, and R. F. Ismagilov. Effects of viscosity on droplet formation and mixing in microfluidic channels. *Analytica Chimica Acta*, 507:73–77, 2004.
- T. M. Tsai and M. J. Miksis. Dynamics of a drop in a constricted capillary tube. *J. Fluid Mech.*, 274:197–217, 1994.
- T. M. Tsai and M. J. Miksis. The effects of surfactants on the dynamics of bubble snap-off. *J. Fluid Mech.*, 348:349–376, 1997.
- H. Wong, C. J. Radke, and S. Morris. The motion of long bubbles in polygonal capillaries. 1. Thin-films. *J. Fluid Mech.*, 292:71–94, 1995a.
- H. Wong, C. J. Radke, and S. Morris. The motion of long bubbles in polygonal capillaries. 2. Drag, fluid pressure and fluid-flow. *J. Fluid Mech.*, 292:95–110, 1995b.

## A MATLAB code to solve for flows in the parallel mixing network

```

function [qw, qo] = networkm(m0, alphain0, pin0, valvesin, cont)
% NETWORKM: calculates flow in a parallel mixing network of m0 units.
% The output arguments qw and qo are the m0+1 outlet water and oil
% volume flow rates. There are three inlets with pressures pin0 and
% oil fractions alphain0, and m0+1 outlets at zero pressure.
% If cont==1, use initial guess saved in file networkmdata.mat, as
% provided by the previous run of networkm. If valvesin==1, the
% effect of menisci in the appropriate links is included.

% The water/oil viscosity ratio, mu, the link resistances, R, and
% index numbers of the links that have menisci, valves, are specified
% internally. If the solution cannot be obtained directly, calculate
% the flow for single phase inputs, then set cont=1, and try the
% required values.

global N L e I O alphain pin pout mu R n valves m

if (length(alphain0)~=3)|(length(pin0)~=3)|(m0<1)|...
    (any(alphain0>1)|(any(alphain0<0)))
    disp('Incorrect input data')
    qw=[]; qo=[]; return
end

alphain = alphain0; pin=pin0;
m = ceil(m0); % number of repeating units
N = 6*m+6; % number of nodes
L = 8*m+5; % number of links
I = 3; % number of inlets
O = m+1; % number of outlets
n = 2*L+N-O-I; % number of unknowns

% The matrix l specifies the 2 nodes joined by each link.
l = zeros(2,L);
l(:,1) = [1; 4]; l(:,2) = [2; 5]; l(:,3) = [3; 7];
l(:,4) = [4; 6]; l(:,5) = [5; 6]; l(:,6) = [6; 8];
l(:,7) = [7; 8];

for k = 2:m
    l(:,7*k-6) = [5*k-6; 5*k-1]; l(:,7*k-5) = [5*k-5; 5*k];
    l(:,7*k-4) = [5*k-3; 5*k+2]; l(:,7*k-3) = [5*k-1; 5*k+1];
    l(:,7*k-2) = [5*k; 5*k+1]; l(:,7*k-1) = [5*k+1; 5*k+3];
    l(:,7*k) = [5*k+2; 5*k+3];
end

```

```

end

l(:,7*m+1) = [5*m-1; 5*m+4]; l(:,7*m+2) = [5*m; 5*m+4];
l(:,7*m+3) = [5*m+2; 5*m+5]; l(:,7*m+4) = [5*m+4; 5*m+5];

for k = 1:m
    l(:,7*m+k+4) = [5*k+3; 5*m+5+k];
end

l(:,8*m+5) = [5*m+5; 6*m+6];

% The sparse matrix e allows us to calculate pressure drops across
% links and total flow rates into nodes as a sparse matrix multiplication.
e=spalloc(N,L,2*L);
for i = 1:L
    e(l(1,i),i) = -1; e(l(2,i),i) = 1;
end

pout = zeros(1,0); % outlet pressures
mu = 0.1;          % water/oil viscosity ratio
R = ones(1,L);    % link resistances
% inlet lines have low resistance
R([1:7:7*m-6 2:7:7*m-5 3:7:7*m-4]) = ...
    0.01*R([1:7:7*m-6 2:7:7*m-5 3:7:7*m-4]);

valves = [];
if valvesin
    % specify links with nonlinear valves
    for k = 1:m
        valves = [valves 7*k-3 7*k-1];
    end
    valves = [valves 7*m+1 7*m+4];
end

if cont
    load networkmdata % load initial guess
    if length(x)~=n
        disp('Stored data is not for this network')
        qw=[]; qo=[];
        return
    end
else
    q = [(1-mean(alphain))*ones(1,L) mean(alphain)*ones(1,L)];
    p = zeros(1,N-0-I); % simple initial guess
    x = [q p];
end

```

```

nitermax = 50; niter=0;

% Newton iteration to get solution
f0=f(x); nf = norm(f0); nf0 = 1e16;
disp(sprintf('Initial error norm is %3.3g',nf))
while (nf>1e-8)&(niter<nitermax)&(nf<nf0)
    nf0 = nf; J = jacobian(x,f0);
    if isempty(J)
        disp('not physical'), return
    end
    dx = -J\f0'; x = x+dx';
    % Modify guess so that oil and water flow in the same direction
    qw = x(1:L); qo = x(L+1:2*L);
    for i = 1:L
        if qw(i)*qo(i)<0
            if abs(qw(i))<abs(qo(i))
                qw(i) = -qw(i);
            else
                qo(i) = -qo(i);
            end
        end
    end
    x(1:L) = qw; x(L+1:2*L) = qo;
    f0 = f(x); nf = norm(f0); niter = niter+1;
    disp(sprintf('New error norm is %3.3g',nf))
end
if (niter<nitermax)&(nf<nf0)
    qw = x(1:L); qo = x(L+1:2*L);
    if any((qw(L-0:L)<0)|(qo(L-0:L)<0))
        disp('not physical')
    else
        output(x); save networkmdata x
    end
else
    disp('not converging')
end

%%%%%%%%%%%%%%%%%%%%%%%%%%%%%%%%%%%%%%%%%%%%%%%%%%%%%%%%%%%%%%%%%%%%%%%%

function f = f(x)
global N L e I 0 alphain pin pout mu R valves

% extract pressures and flow rates and combine with inlet and outlet values
qw = x(1:L); qo = x(L+1:2*L);
p = [pin x(2*L+1:end) pout];

```

```

f =(e*qw')'; f = f(I+1:end-0);
% sum of water flow rates is zero at interior nodes
f1 =(e*qo')'; f = [f f1(I+1:end-0)]; ]
% sum of oil flow rates is zero at interior nodes
f1 = -p*e-(mu*qw+qo).*R; % pressure loss proportional to flow rates
% add in the effect of the valves
qt = qw(valves)+qo(valves); % total volume flow rate
f1(valves) = f1(valves) - fvalves(qt);
f = [f f1];
for i = I+1:N-0
    qw0 = e(i,:).*qw; qo0 = e(i,:).*qo;
    qwplus = qw0(qw0>0); qoplus = qo0(qo0>0);
    % flows into the ith node
    qwminus = qw0(qw0<0); qominus = qo0(qo0<0);
    % flows out of the ith node
    Qw = sum(qwplus); Qo = sum(qoplus); % total flows in
    alpha = Qo/(Qo+Qw+eps);
    % associated oil fraction -- factor of eps to avoid 0/0
    % check to avoid problems associated with zero flow rate
    if length(qominus)<length(qwminus)
        qominus = qo0(qw0<0);
    elseif length(qwminus)<length(qominus)
        qwminus = qw0(qo0<0);
    end
    f1 = qominus-alpha*(qominus+qwminus);
    f = [f f1(1:end-1)];
    % oil fraction equal to alpha in outlet links
end
f1 = qo(1:I)-alphain.*(qo(1:I)+qw(1:I));
% specify the inlet oil fraction
f = [f f1];

```

```

%%%%%%%%%%%%%%%%%%%%%%%%%%%%%%%%%%%%%%%%%%%%%%%%%%%%%%%%%%%%%%%%%%%%%%%%

```

```

function J = jacobian(x0,f0)

```

```

global n L

```

```

% calculate the Jacobian associated with f0 at x=x0.

```

```

del = 1e-8; J = zeros(n,n);

```

```

dir = sign(sign(x0(1:L)) + sign(x0(L+1:2*L)));

```

```

dir = [dir dir ones(1,n-2*L)];

```

```

% we calculate dir to stop the perturbation of x0 changing the sign
% of a flow rate

```

```

for j = 1:n

```

```

    del1 = dir(j)*del;
    x0(j) = x0(j)+del1;
    f1 = f(x0);
    if length(f1)~=n
        J = []; return
    else
        J(:,j) = (f1-f0)'/del1;
        x0(j) =x0(j)-del1;
    end
end
end

%%%%%%%%%%%%%%%%%%%%%%%%%%%%%%%%%%%%%%%%%%%%%%%%%%%%%%%%%%%%%%%%%%%%%%%%

function output(x)
global pin pout L I O N e X Y m
% plot solution
qw = x(1:L); qo = x(L+1:2*L);

alpha = [];
for j=L-O+1:L
    alpha = [alpha qo(j)/(qw(j)+qo(j))];
end figure(100),clf subplot(2,1,1)
plot(1:m+1,qw(end-m:end),'b-x',1:m+1,qo(end-m:end),'r.-')
legend('water','oil',-1),ylabel('outlet volume flow rate') XLim([1
m+1]),xlabel('output number') subplot(2,1,2),plot(1:m+1,alpha,'k.-')
ylabel('oil fraction') xlabel('output number'),XLim([1 m+1])

%%%%%%%%%%%%%%%%%%%%%%%%%%%%%%%%%%%%%%%%%%%%%%%%%%%%%%%%%%%%%%%%%%%%%%%%

function dp = fvalves(qt)
% the pressure drop in links with a meniscus

dQ = 0.0001; % a small factor to give almost a step function.
dp = sign(qt).*(1-exp(-abs(qt)/dQ));

```